MRI Detection of Glycogen and Glucose

J. Ren[1], P. C. van Zijl[2,3], C. K. Jones[2,3], C. R. Malloy[1,4], and A. D. Sherry[1,5]

[1]Advanced Imaging Research Center, University of Texas Southwestern Medical Center, Dallas, Texas, United States, [2]Division of MR Research, Neurosection, Department of Radiology, Johns Hopkins Medical Institutes, Baltimore, MD, United States, [3]F.M. Kirby Center for Functional Brain Imaging, Kennedy Krieger Institute, Baltimore, MD, United States, [4]VA North Texas Health Care System, Dallas, Texas, United States, [5]Department of Chemistry, University of Texas at Dallas, Richardson, Texas, United States

Introduction

Detection of glycogen *in vivo* would have utility in the study of normal physiology and many disorders. Presently, the only MR method available to study glycogen metabolism *in vivo* is ^{13}C MRS [1,2], but this technology is not routinely available on standard clinical scanners. Here, we show that even though the –OH groups of glycogen and glucose are not visible in the physiological proton spectrum, these compounds can be detected indirectly through the water signal using selective radiofrequency (RF) saturation of the hydroxyl protons in the 0.5-1.5 ppm frequency range downfield from water. The resulting saturated spins are rapidly transferred to water protons *via* chemical exchange leading to partial saturation of the water signal, a process known as chemical exchange saturation transfer (CEST). This effect is demonstrated in glycogen phantoms at 9.4T.

Methods

Bovine liver glycogen (Type 1X" G0885 Sigma, CAS# 9005-79-2) was dissolved in water or in phosphate buffered saline (PBS, pH 7.4). The concentration of glycogen is expressed in units of mM glucosyl units with each glucosyl unit contributing 168g/mol. Glucose phantoms of similar molarity were also prepared. Z-spectra of samples in 5 mm NMR tubes were collected on a 9.4T NMR VARIAN spectrometer over a ±10ppm range in steps of 0.1 ppm using a 10s presaturation pulse (B_1 = 1.9 μT), followed by a 2ms crusher and a 90° pulse. TR was 28s, T = 37°C.

Results and Discussion

Figs. 1A,B show ^1H NMR spectra of glycogen in water as a function of added D_2O and temperature, resp. At 4°C, a resonance is visible at 1.2ppm downfield from water, which disappears upon addition of D_2O (Fig. 1A). In 67% D_2O, another exchangeable proton is visible at 0.7ppm, with about half the intensity. These signals are well separated from a single resonance at 0.4 ppm downfield of water, previously assigned to the non-exchangeable $–C_1H$ resonance of the α(1-4') glycosidic linkage [3]. Based on their disappearance in D_2O and their signal intensities, we assign these to the two OH ring protons (C2, C3) and the $-CH_2OH$ sidegroup (C6) in glycogen. The linewidth of the –OH resonance at 1.2 ppm is reasonably sharp at 4°C and broadens when increasing the temperature, characteristic of –OH protons in relatively slow exchange with water protons. In Fig. 1C, so-called Z-spectra are shown as a function of temperature. These spectra reflect the water intensity that remains when saturating at different offsets with respect to the water resonance set at 0ppm. The Z-spectrum at 4°C shows a minor dip at 1.2ppm, which is due to chemical exchange saturation transfer (CEST) effect [4]. Interestingly, while the temperature-based increase in –OH exchange rate reduces visibility in the proton NMR spectra (Fig. 1B), the detection sensitivity is enhanced in the z-spectra (Fig. 1C) due to the dependency of the CEST effect on the proton exchange rate. When using a glycogen solution in PBS buffer, the exchange rate increases dramatically and the -OH resonances are barely visible in the proton spectrum due to severe line broadening (data not shown). However, they are still well visible in the z-spectra, as long as the RF irradiation hits this broadened resonance (intermediate exchange).

To demonstrate that the CEST effect changes with glycogen concentration, Z-spectra were collected for concentrations from 10–200 mM in PBS buffer (Fig. 2A). For comparison, equal concentrations of glucose were also studied (Fig. 2B).Glucose has more exchangeable protons than glycogen and the CEST effect is spread out over a larger range. Although it is evident that the CEST effect becomes more pronounced at higher concentrations, it is difficult to quantify this effect due to the close proximity with regions affected by direct water saturation. The magnitude of this latter effect can be removed in large using a magnetization transfer asymmetry analysis:

$$MTR_{asym}(\Delta\omega) = S(-\Delta\omega)/S_0 - S(\Delta\omega)/S_0$$

where Δω is the frequency offset from water, and *So* and *S* are the water intensities with and without presaturation, resp. Fig. 2C shows that the integrated areas under the MTR_{asym} curves are proportional to concentration, but that the relationship is not strictly linear. This is expected, as the effect can only approach a maximum 100% saturation, which is reached exponentially due to back-exchange of saturated protons. Exact quantitative description of the CEST effect is possible through use of the Bloch equations using a two-compartment model including exchange and RF saturation [5-7].

Figure 1

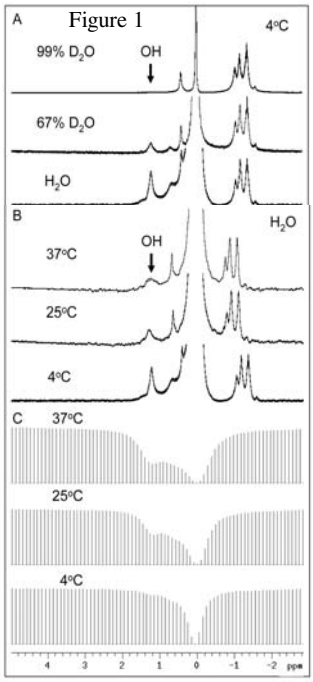

Figure 2

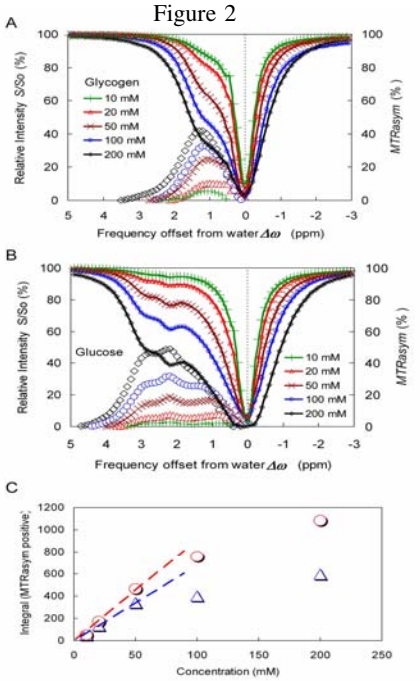

It is of interest to note that, even though the CEST spectra of glycogen and glucose at equivalent concentrations overlap, it will still be possible to study glycogen in many tissues. For instance, given that a typical intracellular concentration of glucose in liver is likely no more than 1-2 mM while that of glycogen in liver from a fed animal is on the order of 200-300 mM. The CEST effect of hydroxyl protons from glycogen may prevail over that from glucose substrate in liver [8].

References

1) Bottomley et al., MRM 12, 348 (1989); 2) Zang et al. Biochem. 29, 6815 (1990); 3) Zang et al., PNAS 87, 1678 (1990); 4) Ward & Balaban, JMR 86, 164 (2000); 5) Zhou et al. MRM 51, 945 (2004); 6) Woessner et al. MRM 53, 790 (2005); 7) McMahon et al. MRM 55, 836 (2006); 8) Jones et al. ISMRM 2006, p482.